

Cavity Optics for Frequency-Dependent Light Squeezing

Natalie Macdonald*

St. Johns University

(Dated: August 1, 2017)

Abstract. In gravitational wave detection, frequency-dependent squeezed light sources will become a method to increase signal sensitivity. This report describes a method to solve an open experimental issue with frequency-dependent squeezing with the use of Python simulation.

1. INTRODUCTION

Squeezing for Improving Sensitivity

Gravitational wave detection is currently limited by different types of noise which hide the signal researchers are trying to obtain. In addition to classical noise, quantum noise of the laser light is still a noise source limiting the detection of gravitational wave signals which researchers are working to surpass. There are two types of quantum noise: quantum shot noise (or QSN) which is related to the uncertainty of the phase measurement, and quantum radiation pressure noise (or QRPN) related to the

*Electronic address: nataliemarie347@gmail.com

uncertainty of the amplitude measurement.

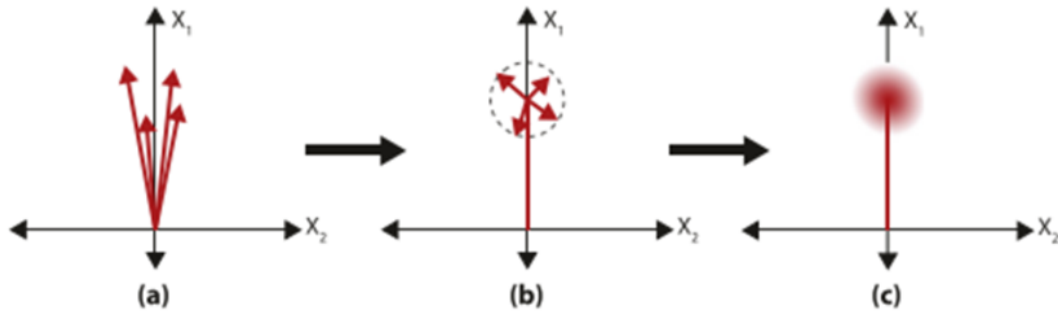


FIG. 1: Visual summation of light noise—Uncertainty of where the light actually is at any point in time can be added together as a vector sum to form a noise ball. Image credit: [Chua et al. (2014)]

Both components of the noise can be squeezed in order to gain a clearer signal-to-noise. That is to say that the noise quadratures can each be reduced by a numerical factor, but not both at the same time. This is a result of the Heisenberg uncertainty principle, which states that both observables cannot be precisely measured at the same time. When maintaining the uncertainty principle one should keep in mind the following equation:

$$\Delta X_1 \Delta X_2 \geq 1 \quad (1)$$

where ΔX_1 represents the phase uncertainty, $\Delta\Phi$; and ΔX_2 represents the amplitude uncertainty, ΔA , so that:

$$\Delta\Phi \Delta A \geq 1 \quad (2)$$

When manipulating the noise ball shown in Figure 1, the uncertainty principle must be respected by adhering to Equation (1). Therefore, when manipulating one of the uncertainties, the other must be adjusted inversely, as in when squeezing the phase uncertainty by a factor of $\frac{1}{S}$, the amplitude uncertainty must be modified by a factor of at least S , as in:

$$\frac{\Delta\Phi}{S} * S\Delta A \geq 1 \quad (3)$$

This conserving factor, S , is considered the "squeezed factor," which means that the other uncertainty is elongated by a corresponding inverse coefficient. Therefore, when one component is squeezed, the other one gets anti-squeezed. This is where one would find frequency-dependent squeezing extremely valuable.

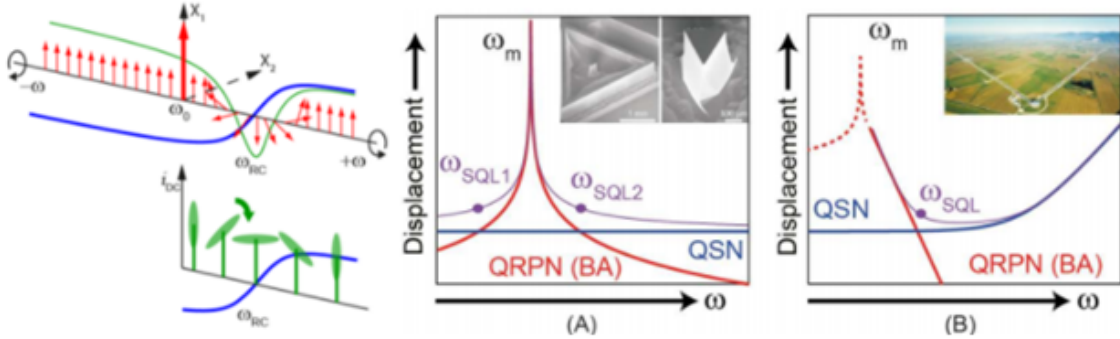


FIG. 2: Rotation of squeezing ellipse for quantum noise reduction—Left: An optical cavity is used to rotate the squeezing ellipse to accommodate noise reduction. (A): Sensitivity curve from an optical micropillar system designed by LKB; micron scale. (B) Similar sensitivity curve containing same types of noise sources from Virgo interferometer gravitational wave detection; kilometer scale. Image credit: [Cohadon, private communication]

From Figure 2, the dominant noise type varies according to frequency. Hence, at

frequencies where the QRPN level is higher, one must squeeze the amplitude noise. Likewise where the QSN is higher, one must squeeze the phase noise that limits displacement.

In order to optimally reduce noise through squeezing, the squeezing angle must rotate according to which kind of noise is targeted at the given frequency. Figure 2 shows the points where the noise types intersect, called the Standard Quantum Limits (SQLs), which show where to switch the angle of squeezing and therefore where to rotate the ellipse.

2. CAVITY OPTICS

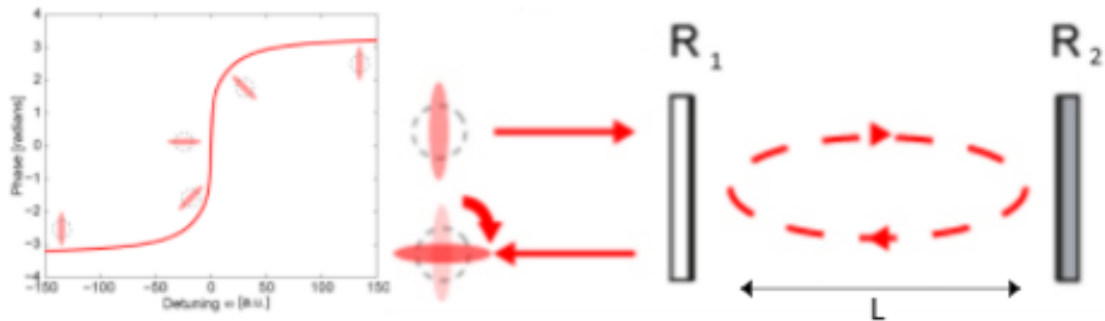
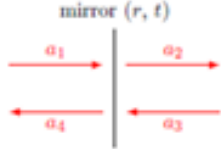


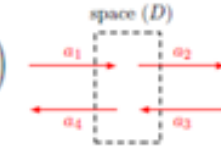
FIG. 3: Fabry-Perot filter cavity for squeezing rotation. Image credit: [Chua]

To perform this rotation, the most developed method is to use a filter cavity such as the Fabry-Perot cavity shown in Figure 3. This kind of system relies on the optical properties of cavities as described in Figure 4 and Figure 5.

This format of left-to-right matrix transformations facilitates the process

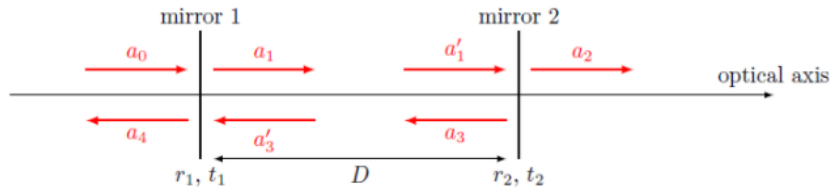
$$\begin{pmatrix} a_1 \\ a_4 \end{pmatrix} = \frac{i}{t} \begin{pmatrix} -1 & r \\ -r & r^2 + t^2 \end{pmatrix} \begin{pmatrix} a_2 \\ a_3 \end{pmatrix}$$


mirror (r, t)

$$\begin{pmatrix} a_1 \\ a_4 \end{pmatrix} = \begin{pmatrix} \exp(ikD) & 0 \\ 0 & \exp(-ikD) \end{pmatrix} \begin{pmatrix} a_2 \\ a_3 \end{pmatrix}$$


space (D)

FIG. 4: Transfer matrices of optical system components—Sets of coupled equations in matrix form that show the transformation of the amplitude vectors from left to right as the field passes through the components.



$$\begin{aligned} M_{\text{cav}} &= M_{\text{mirror1}} \times M_{\text{space}} \times M_{\text{mirror2}} \\ &= \frac{-1}{t_1 t_2} \begin{pmatrix} e^+ - r_1 r_2 e^- & -r_2 e^+ + r_1 e^- \\ -r_2 e^- + r_1 e^+ & e^- - r_1 r_2 e^+ \end{pmatrix} \end{aligned}$$

FIG. 5: Transfer matrix of a two-mirror cavity—This shows that the product of the matrices can simplify to a combined resulting matrix for easier calculation of combined systems. Image credit: [Interferometer Techniques for Gravitational Wave Detection]

of calculating the reflected and transmitted fields resulting from the combination of optical components. The resulting fields of a system of these components can be represented as the product of their corresponding matrices. As in Figure 5, the system of equations can be combined to easily manipulate the components so as to produce custom systems.

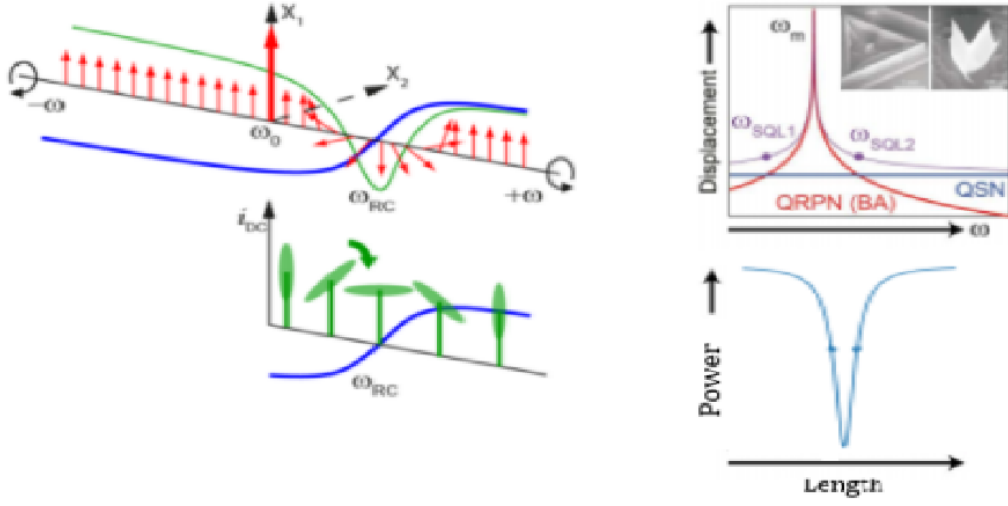


FIG. 6: Squeezing frequency rotation using cavity bandwidths—The rotation cavity changes the angle of the squeezing. This lines up the squeezing so that noise can be optimally reduced between amplitude and phase. Image credit: [Chua]

In order to achieve optimal frequency-dependent squeezing, one must match the full-width, half maximum (or FWHM) of the resonance peak of the beam as it outputs from the rotation cavity to the bandwidth of the SQLs. The FWHM is as follows:

$$FWHM = 2f_p = \frac{2FSR}{\pi} \arcsin\left(\frac{1 - r_1 r_2}{2\sqrt{r_1 r_2}}\right) \quad (4)$$

From this definition, the FWHM depends on the reflectivities and on the length of the cavity (via the Free-Spectral Range(FSR).) Therefore, the filter cavity would need to have the correct parameters to satisfy this SQL bandwidth.

3. PROJECT

Experimental Issue Considered

A filter cavity is necessary to produce an appropriate FWHM to pair with the SQLs of the signal. The rotation of the squeezing is the result of matching the bandwidth of the power output curve to the SQLs in order to optimize the reduction of noise. The issue that arises here is that the locations of the SQL points are dependent on a number of experimental factors which are subject to change. With a two-mirror system, the length and mirrors reflectivity can be chosen in order to acquire the desired FWHM at resonance, but in the anticipation of the experimental factors changing, the reflectivities would have to be adjustable. It is not at all practical to switch mirrors of different reflectivities at the timescales experimental factors change.

Goal and Approach

A solution to this problem is devising a cavity consisting of three mirrors, which could allow for reflectivity-tuning to attain the desired filter cavity bandwidth. The FWHM of the cavity is a function of the reflectivities of the mirrors. As shown in Figure 7, mirrors 1 and 2 can actually be considered one effective mirror because the small cavity produces a transmitted field and a reflected field, just as a single mirror. By adjusting the length of this small cavity, one can change the reflectivity of the black box mirror. This would therefore adjust the FWHM of the filter cavity

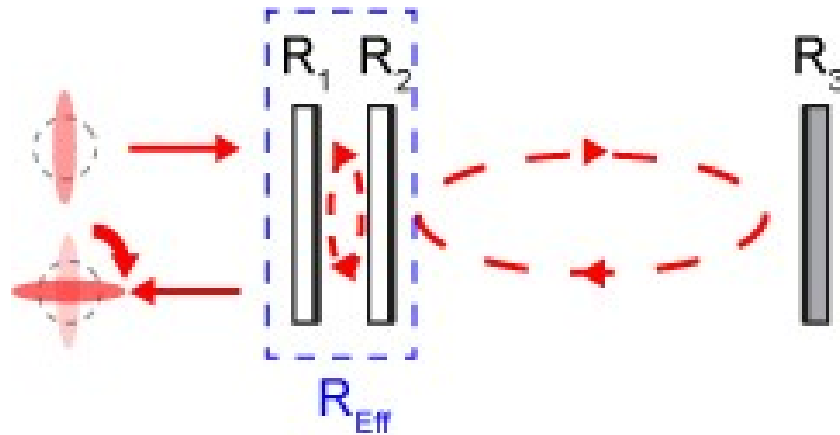


FIG. 7: Three-mirror system to have a filter cavity—Here $R_3 = 1$ for input and output amplitudes on the same side of the system. Image credit: [Chua]

system. My project was to numerically model and verify if such a system performs as expected.

```

58
59  ## Where the left side is [[a_naught],[a11]] ##
60  def mirror_transfer(R):
61
62      r = np.sqrt(R)
63      T = 1-R
64      t = np.sqrt(T)
65
66      mirror_matrix = 1j/t*np.array([[ -1,r],[ -r,r**2+t**2]]) # Multiply by right side. #
67      return mirror_matrix
68
69  def space_transfer(D):
70
71      space_matrix = np.array([[e_plus(D),0],[0,e_minus(D)]])
72      return space_matrix
73
74
75  ## Left to Right Cavity ##
76
77  cavity1_transfer = mirror_transfer(R1).dot(space_transfer(L1)).dot(mirror_transfer(R2))
78
79  whole_cavity_transfer = mirror_transfer(R1).dot(space_transfer(L1)).dot(mirror_transfer(R2)).dot(space_transfer(L2)).dot(
80
81
82
83  # refl = T12/22 #
84  refl_1 = cavity1_transfer[0,1]/cavity1_transfer[1,1]
85  refl_whole = whole_cavity_transfer[0,1]/whole_cavity_transfer[1,1]
86
87

```

FIG. 8: Sample of Python code used to calculate matrices for 5-component system

To compute the reflected and transmitted fields of the three mirror cavity, I worked with the Python program to define matrices for the components of the system, as

per the Cavity Optics section above. A sample of my code is shown in Figure 8. When combined, they produced the Lorentzian resonance peaks of the cavities. When first working with the small cavity, I manipulated the system to see the effect when changing the reflectivity values R_1 and R_2 while varying L_1 . This showed that the resulting transmitted and reflected fields could be manipulated and thus the small cavity could be considered a mirror with adjustable reflectivity.

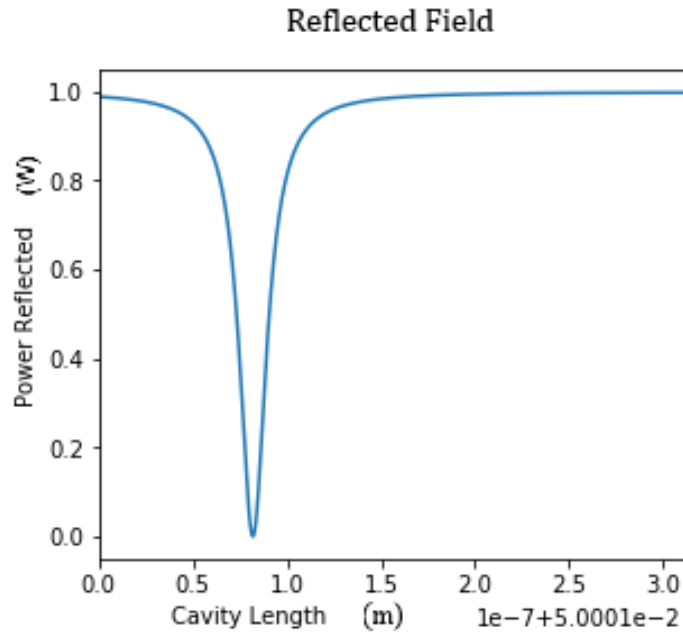


FIG. 9: Plot of Reflected Power vs. Length of small cavity.

Shown in Figures 9 and 10 is the output of my Python code. Again, Figure 9 shows that the reflectivity of the effective mirror can be changed by varying the length of the small cavity. As shown in Figure 10, the phase change, shown by the slope of the phase curve in the middle, can be adjusted by tuning the length of the small

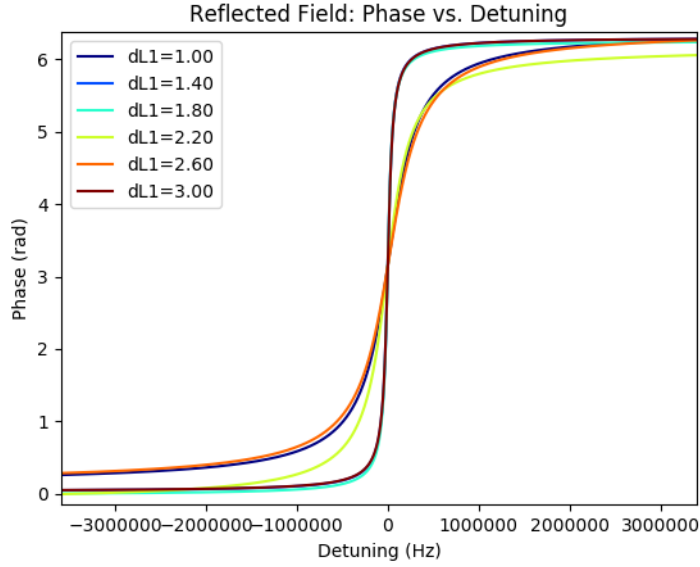


FIG. 10: System phase plot result—shows confirmation that the FWHM of a filter cavity can be manipulated by implementing a three-mirror system.

cavity, thereby changing the reflectivity of the effective mirror. The length of the small cavity for each curve is in the Figure 10 legend.

It is interesting to see that where $dL1$ values are close to resonance, the resulting phase change plots are wider and less steep. This is because when the small cavity approaches its peak, its reflectivity drops and results in a larger FWHM. Therefore these plots do not cross π at resonance on the vertical scale, as simple two-mirror cavities do.

4. SUMMARY

Conclusion

The goal of this project was to verify the feasibility to change the FWHM produced by a filter cavity for frequency-dependent squeezing by implementing a three-mirror system. This is confirmed by Figure 10, because as we can see, the rate of phase change is altered by the length of the small cavity. This means that the FWHM is also changing the point where one could achieve the squeezing rotation. Therefore, we have shown that it is not necessary to change mirrors by hand, and have successfully found a way to adapt the FWHM produced by the full system to match a given SQL bandwidth.

Future work

The next steps for this project include relaxing some of the initial assumptions. For my approach, I chose to set $R_1 = R_2$, so in the future one would look to consider other circumstances. With my assumption, the small cavity is impedance matched with both reflectivities at the same value, but it would be interesting to see how either over- or under-coupling would affect the whole system.

Another assumption I made with my approach was to have a lossless system with $R + T = 1$, so to consider optical losses, as in real world cases, would be needed.

Lastly, I've been considering plane waves for simplicity, but in real world cases, it

would be necessary to consider Gaussian waves, as it is the kind of light beam that is produced by physical lasers and squeezed light sources.

Lastly, we would also need to include using a Pound-Drever-Hall system to control the lengths of the cavity system, so as to be able to adjust to length parameters.

5. ACKNOWLEDGEMENTS

I would like to thank the Optomechanics and Quantum Measurement group at Laboratoire Kastler Brossel for welcoming me so readily into their workplace. I am extremely grateful for the opportunity to be a small part of such a prestigious lab, and thankful for the experience. I'd especially like to thank Dr. Pierre-Francois Cohadon for serving as my advisor, Dr. Sheon Chua for working tirelessly with me through all of my questions, and Dr. Samuel Deléglise for helping with my code. I'd also like to thank Dr. Bernard Whiting, Dr. Guido Mueller, and Ms. Kristin Nichola of the University of Florida—without whom this program would not be possible. Lastly I'd like to thank the National Science Foundation for funding this IREU.

Bibliography

- [1] Bond, C., Brown, D., Freise, A., and Strain, K. (2015). Interferometer Techniques for Gravitational-Wave Detection, arXiv:0909.3661v3 [gr-qc]
- [2] Chua, S. S. Y., Slagmolen, B. J. J., Shaddock, D. A., and McClelland, D. E. (2014). Quantum squeezed light in gravitational-wave detectors. *Classical and Quantum Gravity*, 31(18):183001.